

Multipotent adult progenitor cells can suppress graft-versus-host disease via prostaglandin E₂ synthesis and only if localized to sites of allopriming

Steven L. Highfill,¹ Ryan M. Kelly,¹ Matthew J. O'Shaughnessy,¹ Qing Zhou,¹ Lily Xia,¹ Angela Panoskaltis-Mortari,¹ Patricia A. Taylor,¹ *Jakub Tolar,¹ and *Bruce R. Blazar¹

¹University of Minnesota Masonic Cancer Center and Department of Pediatrics, Division of Bone Marrow Transplantation, Minneapolis

Multipotent adult progenitor cells (MAPCs) are nonhematopoietic stem cells capable of giving rise to a broad range of tissue cells. As such, MAPCs hold promise for tissue injury repair after transplant. In vitro, MAPCs potently suppressed allogeneic T-cell activation and proliferation in a dose-dependent, cell contact-independent, and T-regulatory cell-independent manner. Suppression occurred primarily through prostaglandin E₂ synthesis in MAPCs, which resulted in decreased proinflammatory cytokine produc-

tion. When given systemically, MAPCs did not home to sites of allopriming and did not suppress graft-versus-host disease (GVHD). To ensure that MAPCs would colocalize with donor T cells, MAPCs were injected directly into the spleen at bone marrow transplantation. MAPCs limited donor T-cell proliferation and GVHD-induced injury via prostaglandin E₂ synthesis in vivo. Moreover, MAPCs altered the balance away from positive and toward inhibitory costimulatory pathway expression in splenic T cells and

antigen-presenting cells. These findings are the first to describe the immunosuppressive capacity and mechanism of MAPC-induced suppression of T-cell alloresponses and illustrate the requirement for MAPC colocalization to sites of initial donor T-cell activation for GVHD inhibition. Such data have implications for the use of allogeneic MAPCs and possibly other immunomodulatory nonhematopoietic stem cells for preventing GVHD in the clinic. (Blood. 2009; 114:693-701)

Introduction

The wider application of bone marrow transplantation (BMT) has been limited, in part, by graft-versus-host disease (GVHD) complications. Human and mouse mesenchymal stem cells (MSCs) have been shown to suppress allogeneic-induced and nonspecific mitogen-induced T-cell proliferation in vitro (reviewed in detail^{1,2}). Implicated suppressive mechanisms have included interleukin (IL)-10,³ transforming growth factor (TGF)- β , hepatocyte growth factor,⁴ indoleamine 2,3 dioxygenase (IDO),⁵ nitric oxide,⁶ prostaglandin (PG) E₂,⁷ increased T-regulatory cells (Tregs),⁸ and activation of the PD-1-negative costimulatory pathway.⁹ In vivo, there have been conflicting data regarding the potential of MSCs to suppress GVHD.¹⁰⁻¹²

Multipotent adult progenitor cells (MAPCs) are nonhematopoietic stem cells that can be copurified with MSCs from BM cells. MAPCs express the pluripotent state-specific transcription factors Oct-3/4 and Rex-1, and can differentiate into cell types representative of all 3 germ layers^{13,14}; thus, MAPCs are generally believed to be a more primitive cell type than MSCs. MSCs kept for prolonged periods in culture tend to lose their differentiation capabilities and undergo senescence at approximately 20 to 40 population doublings.^{15,16} In contrast to MSCs, MAPCs have an average telomere length that remained constant for up to 100 population doublings in vitro.¹³ Based upon their differential potential and reduced senescence, MAPCs have been considered as a potentially desirable nonhematopoietic stem cell source for use in allogeneic BMT. In fact, a multicenter phase 1 open label clinical trial of MultiStem, based upon MAPC technology, was initiated in 2008.

In this study, we sought to determine whether MAPCs might be useful for GVHD prevention. We demonstrate that murine MAPCs

are potently immune suppressive in vitro and can reduce GVHD lethality in vivo when present in the spleen, a site of initial allopriming, early post-BMT. Furthermore, we identify the mechanism of action MAPCs use to elicit T-cell inhibition and reduce GVHD-induced tissue injury in vivo.

Methods

Mice

BALB/c (H2^d), C57BL/6 (H2^b; termed B6), and B10.BR (H2^k) mice were purchased from The Jackson Laboratory or the National Institutes of Health (NIH). All mice were housed in a specific pathogen-free facility in microisolator cages and used at 8 to 12 weeks of age in protocols approved by the Institutional Animal Care and Use Committee of the University of Minnesota.

MAPC isolation and culture

MAPCs were isolated from B6 and BALB/c BM, as described.¹³ Briefly, BM was plated in Dulbecco modified Eagle medium/MCDB containing 10 ng/mL epidermal growth factor (Sigma-Aldrich), platelet-derived growth factor-BB (R&D Systems), leukemia inhibitory factor (Chemicon International), 2% fetal calf serum (HyClone), 1 \times selenium-insulin-transferrin-ethanolamine, 0.2 mg/mL linoleic acid-bovine serum albumin (BSA), 0.8 mg/mL BSA, 1 \times chemically defined lipid concentrate, and 1 \times α -mercaptoethanol (all from Sigma-Aldrich). Cells were placed at 37°C in a humidified 5% O₂, 5% CO₂ incubator. After 4 weeks, CD45⁺ and Ter119⁺ cells were depleted using magnetic-activated cell sorting separation columns (Miltenyi Biotec) and plated at 10 cells/well for expansion. For in

Submitted March 30, 2009; accepted May 17, 2009. Prepublished online as *Blood* First Edition paper, May 20, 2009; DOI 1.1182/blood-2009-03-213850.

*J.T. and B.R.B. contributed equally to this work.

The online version of this article contains a data supplement.

The publication costs of this article were defrayed in part by page charge payment. Therefore, and solely to indicate this fact, this article is hereby marked "advertisement" in accordance with 18 USC section 1734.

© 2009 by The American Society of Hematology

vivo experiments in which cells were tracked, MAPCs were used that stably express red fluorescent protein (DSred2) and firefly luciferase transgenes (termed MAPC-DL).¹⁷ For quality control, MAPCs were differentiated into cells representative of the mesodermal lineage, then subjected to in vitro trilineage (endothelium, endoderm, and neuroectodermal) differentiation to ensure multipotency.¹³ MAPCs were analyzed for expression of CD90, Sca1, CD45, CD44, CD13, cKit, CD31, major histocompatibility complex (MHC) class I, MHC class II, CD3, Mac1, B220, and Gr1, and tested for expression of transcription factors Oct-3/4 and Rex-1 by reverse transcription–polymerase chain reaction. Twenty metaphase cells were evaluated by G-banding. Results are found in supplemental Figure 1 (available on the *Blood* website; see the Supplemental Materials link at the top of the online article).

Mixed leukocyte reaction

Lymph nodes (LNs) were harvested from B6 mice and T cells were purified by negative selection using phycoerythrin-conjugated anti-CD19, anti-CD11c, anti–natural killer (NK) 1.1, and anti-phycoerythrin magnetic beads (Miltenyi Biotec). Purity was routinely more than 95%. Spleens were harvested from BALB/c mice, T cell–depleted (anti-Thy1.1), and irradiated (3000 cGy). B6 T cells were mixed at a 1:1 ratio with BALB/c splenic stimulators and plated in a 96-well round-bottom plate (10^5 T cells/well) or in the lower chamber of a 24-well plate Transwell insert (10^6 T cells/well). MAPCs were irradiated (3000 cGy) and plated in a 96-well round-bottom plate (10^4 /well, 1:10) or in a 24-well Transwell plate (10^5 /well, 1:10). Cells were incubated in RPMI 1640 (Invitrogen) supplemented with 10% fetal calf serum, 50 mM 2-mercaptoethanol (Sigma-Aldrich), 10 mM HEPES (N-2-hydroxyethylpiperazine-N'-2-ethanesulfonic acid) buffer (Invitrogen), 1 mM sodium pyruvate (Invitrogen), amino acid supplements (1.5 mM L-glutamine, L-arginine, L-asparagine; Sigma-Aldrich), 100 U/mL penicillin, and 100 mg/mL streptomycin (Sigma-Aldrich). Cells were pulsed with ³H-thymidine (1 μ Ci/well) 16 to 18 hours before harvesting and counted in the absence of scintillation fluid on a β -plate reader. To inhibit PGE₂ production, indomethacin (Sigma-Aldrich) resuspended in ethanol was diluted to reach a final concentration of 5 μ M per flask and incubated overnight at 37°C, 5% CO₂. The next day, cells were trypsinized and washed extensively with 2% fetal bovine serum/phosphate-buffered saline (PBS). Trypan blue exclusion was used to assess effects on live cells. In experiments evaluating the contribution of IDO, 1-methyl-D-tryptophan (1MT; Sigma-Aldrich) was added to the culture media at a concentration of 200 μ M.

Flow cytometry

Purified T cells were stained with 1 μ M carboxyfluorescein-succinimidyl-ester (CFSE; Invitrogen) for 2 minutes and then washed. T cells or CD11c⁺ dendritic cells (DCs) obtained from mixed leukocyte reaction (MLR) cultures were stained for the expression of FoxP3, CD25, CD44, CD62L, CD122, PD-1, PDL1, PDL2, CTLA4, OX40, OX40L, 4-1BB, 4-1BBL, inducible costimulator (ICOS), ICOS-L, CD80, CD86, CD40L, or CD40 antigens. All antibodies were purchased through BD Pharmingen or E-bioscience and stained, according to manufacturer's instructions, and then analyzed using FACSCalibur or FACSCanto (BD Biosciences) and FlowJo software (TreeStar). Calculations to determine the proliferative capacity of T cells were performed, as described.¹⁸

Cytokines and PGE₂ quantification

Quantitative determination of PGE₂ in cell culture supernatants was performed using PGE₂ assay kit (R&D Systems). Quantities of IL-10, TGF- β , IL-2, tumor necrosis factor- α , interferon (IFN)- γ , and IL-12 were determined using Luminex technology (R&D Systems).

In vivo MLR¹⁹

Host BALB/c mice were lethally irradiated using 850 cGy total body irradiation (¹³⁷Cs), followed by intrasplenic (IS) injection of either PBS or 5×10^5 MAPC. The next day, purified T cells were labeled with 1 μ M CFSE and 15×10^6 cells were transferred into stimulator or syngeneic

mice. After 96 hours, spleen and LNs were harvested for fluorescence-activated cell sorter (FACS) analysis.

GVHD

BALB/c recipients were lethally irradiated using 850 cGy total body irradiation on day -1, followed by IS injection of either PBS or 5×10^5 MAPC. On day 0, mice were infused intravenously with 10^7 T cell–depleted donor BM. On day +1, mice were given 2×10^6 purified whole T cells (CD4 and CD8) depleted of CD25. Recipient mice were NK–depleted with anti-asialo GM-1 (WAKO) by intraperitoneal injection of 25 μ L on day -2, a dose previously determined to be effective for depletion of NK cells. Mice were monitored daily for survival and weighed twice weekly as well as examined for clinical GVHD.

Tissue histology

On day 21, GVHD target organs (liver, lung, colon, skin, spleen) were harvested and snap frozen in optimal cutting temperature (OCT) compound (Sakura) in liquid nitrogen. Sections (6 μ M) were stained with hematoxylin and eosin and graded for GVHD using a semiquantitative scoring system (0–4.0 grades in 0.5 increments).²⁰

Immunofluorescence microscopy

Spleens taken from transplanted mice were embedded in OCT, snap frozen in liquid nitrogen, and stored at -80°C. Cryosections (6 μ M) were fixed in acetone for 10 minutes, air dried, and blocked with 1% BSA/PBS for 1 hour at room temperature. Primary antibody was diluted in 0.3% BSA/PBS and incubated for 2 hours. After 3 washes in PBS, sections were incubated with secondary antibody for 45 minutes. Sections were washed and mounted under a coverslip with DAPI (4,6 diamidino-2-phenylindole) antifade solution (Invitrogen) and imaged on the following day at room temperature using an Olympus FluoView 500 Confocal Scanning Laser Microscope (Olympus). Primary antibodies included anti-PGE synthase (Santa Cruz Biotechnology) diluted 1/50 and fluorescein isothiocyanate-conjugated anti-luciferase (Rockland Immunochemicals) diluted 1/100. Goat-Cy3 secondary antibody (Jackson ImmunoResearch Laboratories) was diluted to 1/200.

Bioluminescent imaging studies

A Xenogen IVIS imaging system (Caliper Life Sciences) was used for live animal imaging and imaging of organs taken from transplanted mice. MAPC-DL–bearing mice were anesthetized with 0.25 mL Nembutol (1/10 diluted in PBS). Firefly luciferin substrate (0.1 mL, 30 mg/mL; Caliper Life Sciences) was injected intraperitoneally or added to the media-containing tissues, and imaging was performed immediately after substrate addition. Data were analyzed and presented as photon counts per area.

Statistical analysis

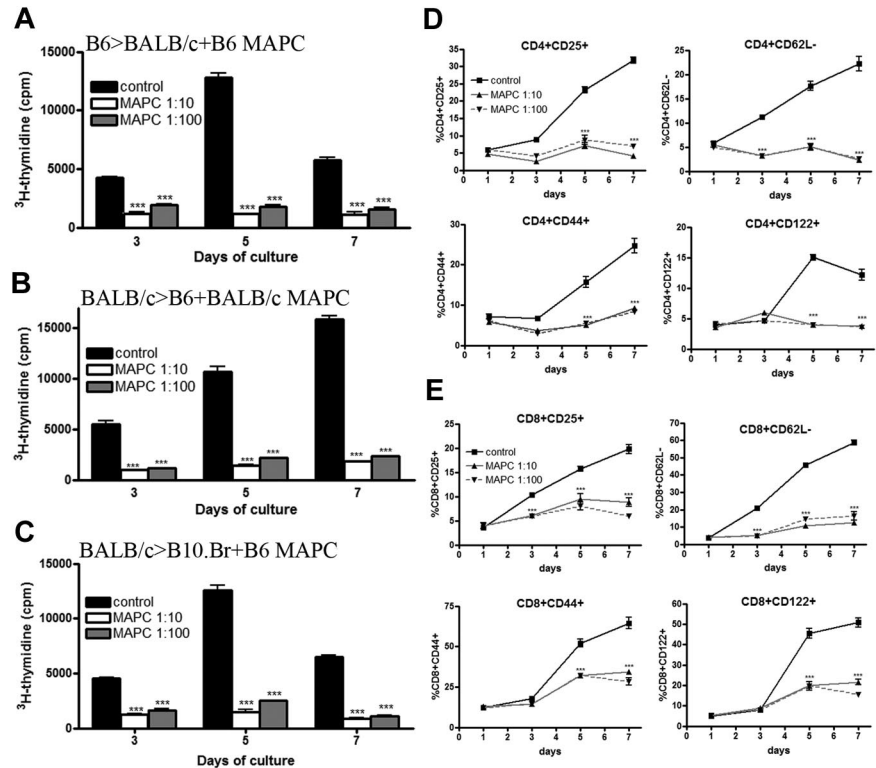
The Kaplan-Meier product-limit method was used to calculate survival curve. Differences between groups in survival studies were determined using log-rank statistics. For all other data, a Student *t* test was used to analyze differences between groups, and results were considered significant if the *P* value was less than or equal to .05.

Results

MAPCs inhibit T-cell proliferation and activation

Murine MAPCs were expanded under low oxygen conditions and had trilineage differentiation potential²¹ (supplemental Figure 1A–B). MAPCs were routinely CD45⁻, CD44⁻, CD13^{low/+}, CD90⁺, *c-kit*⁻, Sca-1⁺, CD31⁻, MHC class I⁻, and MHC class II⁻ (supplemental Figure 1C). Reverse transcription–polymerase chain

Figure 1. MAPCs potently inhibit allogeneic T-cell proliferation and activation. (A) MLR was performed by mixing B6-purified T cells with irradiated BALB/c stimulators (1:1) and B6 MAPCs (1:10, 1:100). These cultures were pulsed with ^3H -thymidine on the indicated days and harvested 16 hours later. Proliferation was determined as a measure of radioactive uptake. MLR reaction was performed as above using BALB/c T cells plus B6 stimulators and BALB/c MAPCs (B), or BALB/c T cells plus B10.Br stimulators and B6 MAPCs (C). FACS analysis of B6 > BALB/c MLR plus B6 MAPCs was performed on the indicated days and gated on CD4⁺ T cells (D) or CD8⁺ T cells (E) in conjunction with activation markers.



reaction expression analysis confirmed that these MAPCs expressed Oct-3/4 and Rex-1 (supplemental Figure 1D). These distinctive characteristics of MAPCs (trilineage differentiation potential, expression of Oct-3/4 and Rex-1, and unique surface phenotype) distinguish them from other similar, less primitive cell types such as MSCs. G-banding analysis revealed that 90% of the 20 metaphase cells analyzed had a normal karyotype (supplemental Figure 1E). The remaining 2 cells had a tetraploid complement, one with an additional deletion within the long arm of chromosome 6. The tetraploid complement is within the normal limits for cultures that have been passaged several times. The finding of a single cell with a structural abnormality is considered a nonclonal event, and this cytogenetic study was interpreted as normal.

We have previously reported that MAPCs do not stimulate a T-cell alloresponse even when MAPCs have been pretreated with IFN- γ to up-regulate MHC class I, intracellular adhesion molecule-1, and CD80 expression.²² These studies did not address the possibility that MAPCs could actively suppress an immune response. To explore this possibility, B6 MAPCs were mixed with purified B6 T cells and added to irradiated BALB/c stimulators. A significant reduction in proliferation was observed in MAPC-treated MLR at all time points (Figure 1A). On the peak of the response (day 5), there was a near-complete inhibition of T-cell alloresponses from MAPC cocultures (91%, $P < .001$ for 1:10; and 86%, $P < .001$ for 1:100). To ensure the observed inhibitory effect was not dependent on this specific MAPC isolate or B6 strain of MAPC, BALB/c-derived MAPCs were generated and mixed with BALB/c T cells and B6-irradiated stimulators. The percentage of T-cell inhibition on the day of peak response was 88% ($P < .001$) for 1:10 cocultures, and 85% ($P < .001$) for 1:100 cocultures (Figure 1B). These data indicated that the MAPC immune-suppressive properties are not dependent on isolate or strain. The presence of MAPCs in MLR cultures significantly reduced the percentage of activated (CD25⁺, CD44^{high}, CD62L^{low}, CD122⁺) CD4⁺ (Figure 1D) and CD8⁺ (Figure 1E) T effectors on days 5 and

7 ($P < .001$ for both time points for 1:10 and 1:100 cocultures). Taken together, the data show that MAPCs potently inhibit the activation and proliferation of alloresponsive T cells in vitro.

To determine whether suppression was MHC restricted, B6 MAPCs were added to purified BALB/c T cells and irradiated B10.Br splenic stimulators (Figure 1C). Third-party MAPCs potently inhibit allogeneic T-cell proliferation (89% and 80% average T-cell inhibition at peak for 1:10 and 1:100, respectively; $P < .001$ for both), indicating inhibition was not MHC restricted. To determine whether MAPCs had differential effects on resting versus actively proliferating T cells, MAPCs were added on days 0, 1, 2, and 3 to a MLR consisting of B6 T cells and BALB/c stimulators. On both days 5 and 7, T-cell proliferation was significantly diminished by MAPCs ($P < .001$; supplemental Figure 2A), indicating that MAPCs can suppress an ongoing alloresponse.

Several studies attribute the T-cell inhibitory properties of MSCs to their ability to generate or regulate Tregs.^{8,23,24} MLR-MAPC cocultures were performed using T cells or CD25-depleted T cells to determine whether the lack of Tregs at the priming stage of the allogeneic response would impact MAPC-induced suppression. No difference was seen in the suppression potency between Treg-depleted versus replete cultures (Figure 2A). Foxp3⁺Treg percentages did not increase in MAPC versus control cultures through all time points (day 5 shown) in cultures using CD25-replete versus depleted T cells (Figure 2B-C and data not shown). We conclude that MAPC-mediated suppression neither depends upon Tregs in the responding T-cell fraction nor induces Tregs from the CD25⁻ T-cell fraction.

Murine MAPCs mediate suppression via PGE₂

MSCs are known to be capable of suppressing immune responses via release of soluble factors. To determine whether MAPCs could act similar to MSCs, we used a Transwell coculture system in which B6 T cells and BALB/c splenic stimulators were placed in

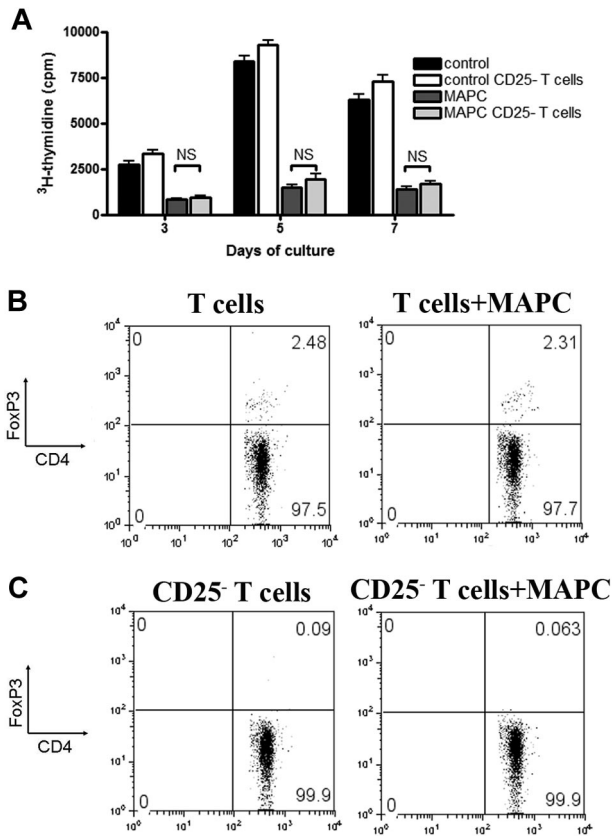


Figure 2. MAPC-mediated suppression in vitro is independent of Tregs. B6 > BALB/c MLR culture was performed using purified T cells or T cells that were CD25-depleted and MAPCs at 1:10 ratios. ³H-thymidine was added on the indicated days, and proliferation was measured (A). FACS analysis was performed on day 5 on the non-CD25-depleted (B) and the CD25-depleted (C) MLR cocultures to determine the percentage of CD4⁺FoxP3⁺ T cells.

the lower chamber and B6-derived MAPCs were placed in the upper chamber of a Transwell. MAPCs inhibited T-cell alloresponses in a contact-independent manner (Figure 3A), producing an 85% inhibition of T-cell proliferation on day 5 ($P < .01$). No significant differences were seen due to the presence of a Transwell ($P = .19$). To prove that MAPC-derived soluble factors were necessary and sufficient to induce immune suppression, cell-free

supernatant from untreated and MAPC-treated MLR cocultures was added in a 1:1 ratio with fresh media to a second MLR primary coculture. MAPC-treated supernatant was equally as effective in inhibiting T-cell proliferation as MAPCs placed in direct contact with responders (Figure 3B; $P = .20$). Supernatants were taken from B6 > BALB/c MLR cultures, and enzyme-linked immunosorbent assays were performed to determine effects on proinflammatory cytokine secretion. MAPCs decreased proinflammatory cytokine (tumor necrosis factor- α , IL-12, IFN- γ , and IL-2) concentrations within these cultures at all time points (Figure 3C). Although no significant increases in the amount of anti-inflammatory cytokines, IL-10, or TGF- β were observed, there was a significant increase in PGE₂ concentrations within MAPC cocultures ($P < .001$; Figure 3D).

To determine whether MAPCs were the source of PGE₂ and whether the increase in PGE₂ was responsible for decreased T-cell alloresponsiveness, MAPC expression of PGE₂ synthase was verified, indicating they were capable of converting PGH₂ into PGE₂ (supplemental Figure 3A). Moreover, analysis of supernatant taken from MAPC cultures alone had increased concentrations of PGE₂ (8113 ± 615 pg/mL at day 3; 7591 ± 700 pg/mL at day 5; data not shown). This indicated MAPCs are capable of producing PGE₂ constitutively without the need for allostimulation. Overnight treatment of MAPCs with the cyclooxygenase 1/2 inhibitor, indomethacin, potently inhibited the upstream synthesis of PGE₂ for the period of the MLR culture (9 days; supplemental Figure 3B) without adversely affecting MAPC viability (data not shown). When indomethacin-treated MAPCs were added to MLR cocultures, they no longer inhibited T-cell alloresponses (Figure 4A). At the peak of the response (day 6), there was a 90% versus 13% inhibition in allogeneic T-cell proliferation when untreated versus indomethacin-pretreated MAPCs were in coculture ($P < .001$). At all other days examined, pretreatment of MAPCs with indomethacin led to more than 90% restoration of proliferation.

MAPCs were found to up-regulate IDO upon activation with IFN- γ (data not shown). To determine whether IDO could account for the remaining inhibitory properties of these cells (~10%), MAPCs were pretreated with indomethacin and/or the MLR coculture was treated with IMT, a competitive inhibitor of IDO. The addition of IMT to MLR cocultures did not increase T-cell proliferation (supplemental Figure 3C), and there was little/no

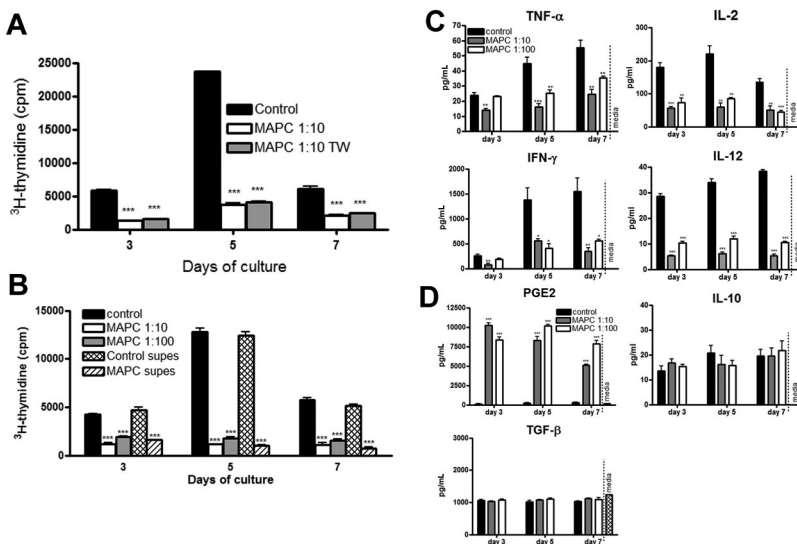


Figure 3. MAPCs mediate suppression via a soluble factor. B6 > BALB/c MLR plus MAPCs at 1:10 ratio was arranged by placing T cells and stimulators in the lower well of a Transwell insert and MAPCs in the upper chamber, or by placing MAPCs in direct contact with stimulators and responders (A). (B) Supernatant taken from MAPC or control cocultures on day 3 was added in 1:1 ratio with fresh media to a B6 > BALB/c MLR. Results of MAPCs at 1:10 and 1:100 ratios in direct contact with responding T cells are shown for comparison. Proliferation was assessed using ³H-thymidine uptake. Enzyme-linked immunosorbent assay was performed on MLR supernatant harvested on the indicated day to determine the amount of proinflammatory (C) and anti-inflammatory (D) cytokines in culture with MAPCs at 1:10 and 1:100 ratios.

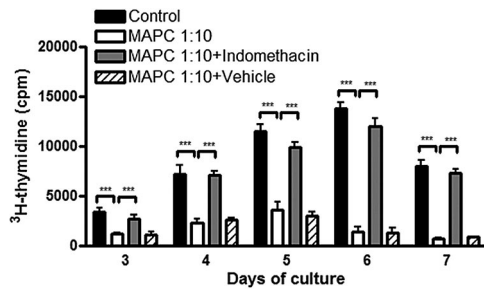


Figure 4. MAPCs inhibit T-cell alloresponses through the secretion of PGE₂. B6 > BALB/c MLR cultures were arranged as before. MAPCs, either untreated, treated overnight with 5 μM indomethacin to inhibit production of PGE₂, or treated with vehicle, were titrated in at 1:10 ratios. Proliferation was assessed as above (panel A).

additive effect of indomethacin pretreatment of MAPCs with IMT treatment of the coculture (supplemental Figure 3C).

Murine MAPCs can delay GVHD mortality and target tissue destruction if localized to the spleen early post-BMT

The prophylactic anti-GVHD efficacy of MAPCs was tested in lethally irradiated BALB/c mice given B6 BM plus 2 × 10⁶ B6 CD25-depleted T cells. Due to the lack of expression of MHC class I molecules on MAPCs, host mice were NK cell-depleted on day -2 using anti-asialo GM-1 so as to ensure MAPCs were not rejected early posttransplant. Cohorts were given MAPC-DL or PBS via intracardiac (IC) injections directed toward the left

ventricle, which allows for direct access to the systemic circulation and to a more widespread biodistribution and longer persistence of MAPC-DLs.²² Despite their potent suppressive capacity *in vitro*, MAPC-treated mice versus control mice had virtually identical survival rates (Figure 5A). Bioluminescent imaging (BLI) of these mice revealed that most T cells had migrated to BM cavities (skull, femur, spine), rather than to T-cell priming sites such as LNs or spleen (data not shown).

With the known short half-life of PGE₂ *in vivo*,²² we speculated that sufficient quantities of this molecule might not be penetrating T-cell allopriming sites such as LNs and spleen. Subsequent studies were performed in which untreated or indomethacin-treated B6 MAPCs were given via an IS injection. IS administration of MAPCs was performed before the infusion of T cells to allow time for MAPC conditioning of the splenic microenvironment. Controls were given BM alone plus sham surgeries or BM plus T cells and sham surgeries. BLI imaging of mice given MAPC-DL IS showed that these cells remained within the spleen for a period of up to 3 weeks (supplemental Figure 4A-B). Although we are unsure of the mechanisms responsible for MAPC sequestration within the spleen for long time periods after IS injection, we speculate that either they do not have direct access to vessels within the spleen, which would allow them to return to circulation and home back to the BM as in the IC model, or alternatively, there may be an unfavorable chemokine gradient within the splenic microenvironment that prevents migration of MAPCs from the spleen. With respect to the latter, it is known that stromal derived factor-1 (CXCL12) is

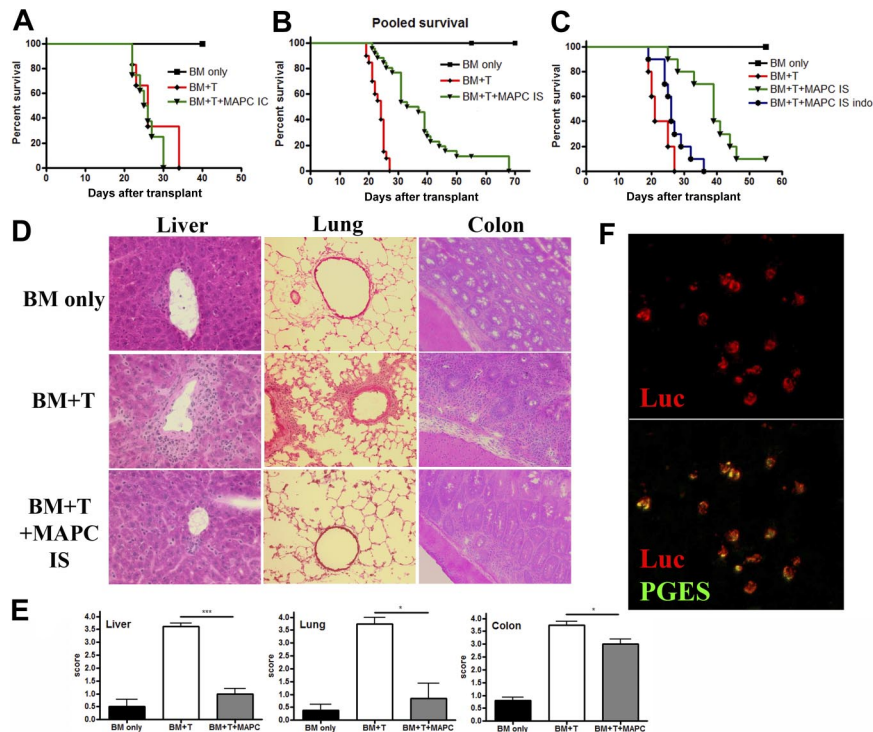


Figure 5. The capacity of MAPCs to delay GVHD mortality and limit target tissue destruction is dependent on anatomic location of the cells and their production of PGE₂. BALB/c mice were lethally irradiated and then given 10⁶ BM cells from B6 mice on day 0, followed by 2 × 10⁶ purified CD25-depleted whole T cells on day 2. On day 1, mice were given 5 × 10⁵ untreated B6 MAPCs or PBS delivered via IC injections. Kaplan-Meier survival curve is representative of 1 experiment in which BM only and BM plus T group had n = 6, and MAPC group had n = 8 (A). (B) BMT was performed as in panel A, except mice were given PBS or 5 × 10⁵ MAPC IS on day 1. The survival curve is representative of 3 pooled experiments (BM only, n = 18; BM + T, n = 20; MAPCs, n = 26; MAPCs vs BM + T, P < .001). (C) Survival curve representative of 1 experiment in which mice received BMT plus untreated MAPCs or MAPCs pretreated overnight with indomethacin before IS injection (BM only, n = 5; BM + T, n = 5; MAPCs, n = 10; MAPC indo, n = 10; MAPCs vs MAPC indo, P = .002). Tissue taken from cohorts of mice from panel B was harvested on day 21 and embedded in OCT, followed by freezing in liquid nitrogen. Sections (6 μM) were stained with hematoxylin and eosin and analyzed for histopathologic evidence of GVHD. Representative images are shown. (D) Magnification × 200. (E) The average GVHD score for BM only, BM plus T, and BM plus T plus MAPC (IS) cohorts is shown. (F) Spleens were harvested from BMT plus MAPC IS transplanted mice on day 21 and snap frozen in OCT compound. Tissue sections were cut and stained using anti-luciferase and anti-PGE synthase antibodies. Confocal analysis reveals that MAPCs are found in the spleen at this time point and retain their ability to produce PGE₂. (F) Top shows luciferase alone, and bottom shows colocalization of PGE synthase with luciferase.

up-regulated in the spleen of mice after total body irradiation,²⁵ and we have demonstrated that MAPCs express the receptor for this molecule (CXCR4; our unpublished observations). This interaction, therefore, may be responsible for the observed retention of MAPCs within the spleen. Compared with controls receiving BM plus T cells plus sham surgeries, mice given IS injections of untreated MAPCs have a significant improvement in survival ($P < .001$), with 2 long-term survivors greater than 55 days (Figure 5B). MAPC-DLs present in the spleen continued to express PGE synthase, as shown by costaining (Figure 5F). Therefore, although it is possible that some MAPCs may have undergone differentiation in vivo in this setting, they are still able to produce PGE₂ as late as 3 weeks after transplant. Indomethacin pretreatment of MAPCs precluded their protective effect (Figure 5C; MAPC vs MAPC-Indo, $P = .0058$), indicating that PGE₂ is responsible for the suppressive potential of these cells in vivo. Mean body weights of these mice recapitulate these findings (supplemental Figure 4C). On day 21 post-BMT, there were significantly more infiltrating lymphocytes in the liver and lung, resulting in increased necrotic foci and perivascular and peribronchiolar cuffing (Figure 5D-E) along with large numbers of infiltrating lymphocytes in the colons of GVHD control- versus MAPC-treated mice (Figure 5D-E).

Therefore, MAPCs use PGE₂ as a mechanism in vivo that leads to a significant increase in survival of mice with GVHD, and importantly, these effects were dependent upon MAPC location.

MAPCs diminish T-cell proliferation and activation within the local environment

The direct in vivo effects of PGE₂ on donor T-cell proliferation and activation using the MAPC IS administration model were determined. BALB/c mice were lethally irradiated and given B6 MAPC-DL via IS injections on day 0, and B6 CFSE-labeled CD25-depleted T cells (15×10^6) on day 1. Controls were given labeled T cells alone plus sham injection. On day 4, LNs and spleens were analyzed by BLI. MAPCs were only located within the spleen and had not migrated out to the LNs (supplemental Figure 5A). FACS analysis was performed to determine the percentage of T cells that had divided during this time period, and the proliferative capacity (the number of daughter cells that each responder cell produced) was calculated. There was a significantly reduced number of CD4⁺ and CD8⁺ T cells that had undergone cellular division, as determined by CFSE dilution in MAPC-treated versus control groups (Figure 6A). In the LNs of the same mice, there were no significant differences in either CD4⁺ or CD8⁺ T cells that had undergone cellular division. MAPCs resulted in a significantly reduced proliferative capacity of CFSE-labeled CD4⁺ and CD8⁺ T cells in the spleen (Figure 6B). Each alloreactive CD4 T cell that had divided gave rise to 15 versus 10 daughter cells in untreated versus MAPC-treated mice ($P = .0005$). Each alloreactive CD8 T cell that divided gave rise to 10 versus 6 daughter cells, respectively ($P = .0004$; Figure 6B). In the LNs of the same mice, there were no significant differences in CD4⁺ or CD8⁺ T-cell proliferative capacity between control- and MAPC-treated mice (Figure 6C). Each CD4⁺ T cell gave rise to an average of 9 and 9.4 daughter cells ($P = .25$), and each CD8⁺ T cell gave rise to 6.8 and 7.3 daughter cells in untreated versus MAPC-treated groups ($P = .061$). More splenic T cells down-regulated CD62L and up-regulated CD25 in the control- versus MAPC-treated group (Figure 6D). In LNs, no such effects were observed (Figure 6E), indicating that MAPCs limit allogeneic T-cell activation and expansion locally in vivo. Others have shown that PGE₂ can influence the expression of costimulatory molecules.²⁶ Therefore,

we tested T cells and DCs within this in vivo MLR setting using treated or untreated MAPCs to determine whether the PGE₂ effect on proliferation was due to its influence on costimulatory molecule expression. There were significantly more CD4⁺ and CD8⁺ T cells within MAPC-treated groups than the control groups that expressed the negative costimulatory molecules PD-1 on CD4⁺ and CD8⁺ T cells (Figure 7A-B). Similarly, CTLA-4 was also expressed on a higher percentage of CD4⁺ and CD8⁺ T cells in MAPC versus control cultures. Also consistent with MAPC-induced suppression, the percentage of OX40⁺CD8⁺ T cells was significantly lower than controls, along with a trend toward less OX40 and 4-1BB expression on CD4⁺ and CD8⁺ T cells, respectively. These effects were reversed using MAPCs treated with indomethacin before in vivo administration (Figure 7). Within the MAPC versus control groups, there was a significant increase in the percentage of DCs expressing PD-L1 and CD86 (Figure 7C) without significant differences in the percentage of DCs expressing other costimulatory molecules (Figure 7C). When using indomethacin-treated MAPCs, again, these effects were mostly reversed. There were no significant differences in the percentages of T cells and antigen-presenting cells expressing ICOS, ICOS-L, CD40, and CD40L between groups (data not shown). Taken together, these data indicated that PGE₂ accounts for the majority of the suppressive potential of MAPCs and has the downstream effect of increasing the percentage of cells expressing negative costimulatory regulators (PD1, PDL1, CTLA4), and decreasing the percentage of cells expressing positive costimulatory regulators (OX40, 4-1BB).

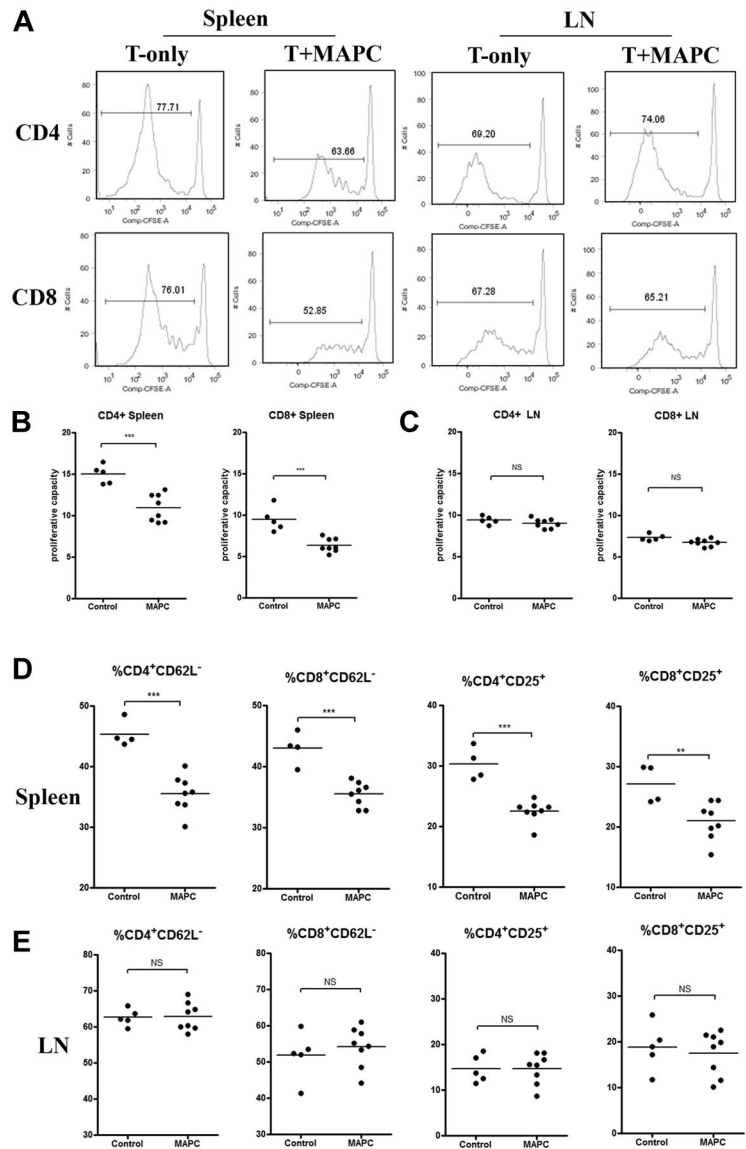
Discussion

We have shown that MAPCs inhibit the proliferation and activation of allogeneic T cells via the elaboration of PGE₂. In vivo, MAPCs did not home to lymphoid organs and were incapable of suppressing GVHD. Despite the contact independence of MAPCs in suppressing alloresponses in vitro, MAPCs reduced GVHD only when injected into the spleen. MAPC synthesis of PGE₂ in situ resulted in an unfavorable in vivo environment for supporting T-cell activation. These data emphasize the importance of ensuring homing of immunomodulatory cell types to relevant tissue sites to dampen T-cell priming and subsequent tissue injury.

In this study, we show that MAPCs are constitutive producers of PGE₂. Inhibiting MAPC synthesis of PGE₂ by treatment of the cells with a potent cyclooxygenase inhibitor restored in vitro T-cell proliferation in an allo-MLR culture to more than 90% of the control. In contrast, precluding other known inhibitors of an immune response, IL-10, TGF- β , or IDO, using IL-10 receptor knockout T cells, anti-TGF- β antibodies, or the competitive IDO inhibitor, 1MT, did not affect T-cell proliferation in MLR cultures (supplemental Figure 3C and data not shown). Thus, of the several known soluble factors that have been shown to contribute to the suppression of T cells in MLR cultures in noncontact systems, PGE₂ appears to be the dominant secreted molecule involved in MAPC-induced suppression of an in vitro alloresponse. Similarly, in vivo, inhibition of GVHD required MAPC production of PGE₂ in situ.

PGE₂ can be produced by many cells²⁷ and influence the function of a wide array of immune cells, including T cells,²⁸ B cells,²⁹ macrophages,³⁰ and DCs.³¹ MAPC synthesis of PGE₂ in vitro was associated with the up-regulation of negative costimulatory molecules and down-regulation of positive costimulatory molecules on T cells and antigen-presenting cells (data not shown). In contrast, a recent report has shown that human monocyte

Figure 6. MAPCs dampen T-cell proliferation and activation within the local environment. In vivo MLR was performed by administering lethally irradiated BALB/c mice with 5×10^5 B6 MAPCs IS (day 0), followed by 15×10^6 B6 CFSE-labeled CD25-depleted T cells (intravenously; day 1). Control mice were given labeled T cells alone plus sham surgeries. Spleens and LNs were harvested on day 4 and analyzed via FACS for CD4 and CD8 expression and percentage of CFSE dilution (A). The proliferative capacity for CD4⁺ and CD8⁺ T cells in the spleen (B) and LNs (C) of transplanted mice was calculated, as previously published.¹⁸ (D-E) Activation markers for CD4⁺ and CD8⁺ T cells in the spleen and LNs were analyzed using FACS and graphed.



(CD14⁺) and myeloid (CD11c⁺) DCs up-regulate positive costimulatory molecules (OX40L, CD70, 4-1BBL) if PGE₂ is added during the maturation process.³² We speculate that the apparent discordance may be due to the differences in the maturation status of the DCs at the time of PGE₂ stimulation, although neither DC location (BM vs spleen) nor species-specific differences can be excluded as explanations. PGE₂ is known to have both stimulatory and inhibitory effects on DC activation, dependent upon the context in which PGE₂ is encountered. DCs encountering PGE₂ in the periphery have an increased activation and increased migratory abilities, whereas those encountering PGE₂ within secondary lymphoid organs lead to decreased activation and decreased effector function.³¹

In this and our prior report,²² we have shown that donor MAPCs preferentially migrated to the BM after systemic delivery, and are thus unlikely to directly interact with GVHD-causing donor T cells within lymphoid organs. Because the half-life of PGE₂ in vivo is extremely short (~ 30 seconds),³⁴ we hypothesized that this mechanism of MAPC-mediated suppression may not penetrate secondary lymphoid organs to a sufficient degree to inhibit T-cell activation and proliferation. MAPCs used in our studies did not express CD62L or CCR7, important for homing to secondary lymphoid

organs (data not shown). To circumvent this problem, MAPCs were delivered directly into the spleens at the time of BMT, thereby restoring the capacity of MAPCs to suppress donor T-cell activation and proliferation in vivo. As predicted, this MAPC-mediated effect was only observed in the spleens and not in the LNs of transplanted mice (Figure 6), confirming our initial hypothesis that PGE₂ acts in a local manner. This suppressive effect on donor T cells in vivo improved the survival of mice experiencing severe GVHD, a process that was almost entirely dependent on PGE₂ production from MAPCs (Figure 5B-C). Although the overall survival was improved by MAPC injection into the spleen, most mice eventually succumbed to the disease with only a minority becoming long-term survivors. Therefore, although approximately 8-fold more T cells migrate to the spleen than to LNs during a given time point,³⁵ T-cell activation within the LNs is sufficient, possibly along with residual T-cell activation within the spleen, to cause lethal GVHD. The importance of secondary lymphoid organs for GVHD initiation can be derived from studies in which mice that lack all secondary lymphoid organs are incapable of developing severe GVHD.^{36,37} Because studies have shown that GVHD cannot be prevented by host splenectomy alone,³⁸ our data suggest that MAPC-mediated suppression of donor T cells within the spleen is

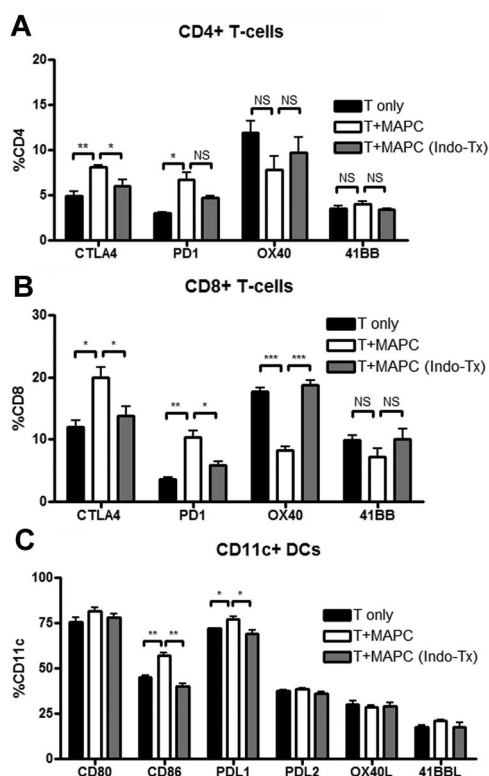


Figure 7. MAPCs affect costimulatory molecule expression on T cells and DCs in the spleen. FACS analysis of spleen cells harvested from transplanted mice on day 4 was performed to determine the percentage of CD4⁺ (A), CD8⁺ (B), and CD11c⁺ (C) cells that expressed the indicated costimulatory molecules. In this transplant, MAPCs were untreated or pretreated with indomethacin, as described, before their application.

not equivalent to a splenectomy. This may be due to the functional alterations of donor T cells that are exposed to PGE₂ within the spleen in lymphoid-replete recipients in contrast to the unrestrained activation and proliferation of a higher number of donor T cells that would traffic to the LNs of splenectomized hosts. Interestingly, MAPCs suppressed GVHD-induced tissue injury to a greater extent in the liver and lung compared with the colon. Whether the influence of MAPCs on donor splenic T-cell function, as evidenced by the pattern of costimulatory molecule expression or the homing of donor T cells after exposure to MAPCs in the spleen, would favor preferential organ targeting is unknown.

The requirement for homing of immune-suppressive cells to secondary lymphoid organs to exert their maximum biologic effect is not unique to MAPCs. For example, previous studies using murine BM-derived MSCs have proven to be ineffective in altering GVHD lethality.¹² For Treg-induced suppression of GVHD, high levels of CD62L expression were needed for optimal *in vivo* suppression of GVHD-induced lethality, although not for *in vitro* suppression.^{39,40} Whereas CCR5 expression on Tregs was not required for *in vitro* suppression, CCR5 knockout Tregs were inferior to wild-type Tregs in suppressing GVHD lethality *in vivo*, which was associated with a reduced accumulation of Tregs in lymphoid and nonlymphoid GVHD target organs beyond the first week post-BMT.⁴¹ In solid organ allograft studies, Treg suppression of graft rejection requires the migration of Tregs from the blood to the allograft to the draining LNs.⁴² We conclude that the kinetics and homing patterns of immune modulatory cells to the sites of alloresponse are critical in determining the outcome of an alloresponse to foreign antigens, and that GVHD inhibition by MAPCs requires homing to lymphoid sites that support GVHD initiation.

Although recent reports indicate that MAPCs can modify injury induced by vascular ischemia,⁴³⁻⁴⁵ the *in vitro* and *in vivo* immunosuppressive properties of MAPCs to date are largely undefined. To our knowledge, only one recent report has described the immunosuppressive potential of rat-derived MAPCs.⁴⁶ Similar to our results, rat MAPCs inhibited alloresponses via a contact-independent mechanism. In contrast to our results, rat MAPC-induced inhibition of T-cell alloproliferation *in vitro* was dependent upon IDO expression because IMT reverses the suppressive effects of rat MAPCs. Furthermore, rat MAPCs expressed MHC class I antigens, in distinction to both human- and mouse-derived MAPCs that are targeted by NK-mediated lysis.²² Although neither the homing receptor expression nor the *in vivo* homing or suppressor cell mechanisms responsible for GVHD inhibition were reported, similar to our study, MAPCs were effective in reducing GVHD lethality.

In summary, this is the first study to demonstrate the *in vitro* and *in vivo* immune-suppressive capacity and mechanism of MAPCs in preventing GVHD. The direct demonstration that PGE₂ secretion is able to mediate donor T-cell suppression suggests a mechanism by which other cell types such as MSCs and myeloid-derived suppressor cells may be able to suppress adverse alloresponses *in vivo*.⁴⁷ Furthermore, these data suggest that pharmacologic strategies toward achieving sufficient PGE₂ concentrations in relevant target organs during the acute initiation phase may be useful for GVHD prevention. Importantly, this is also the first study to demonstrate that location of MAPC immune-suppressive, nonhematopoietic stem cells *in vivo* to lymphoid organs is a critical determinant of the efficacy of GVHD prevention. Future approaches to ensure the targeting of immune-suppressive cells to allopriming sites may increase the efficacy of both nonhematopoietic stem cells and other immune-suppressive populations with promise to inhibit GVHD.

Acknowledgments

We thank Dr Christine Vogtenhuber, Dr Christoph Bucher, Rachel Veenstra, Emily Goren, and Ronald McElmurry for helpful discussions and technical assistance. We also thank the University of Minnesota cytokine reference laboratory and Sophia Christoforides for technical assistance with cytokine analysis.

This work was supported in part by NIH grants R01 AI34495, HL56067, and HL49997 (Bethesda, MD; to B.R.B.), and the Children's Cancer Research Fund (Minneapolis, MN; to S.L.H.).

Authorship

Contribution: S.L.H. designed, organized, and supervised research, performed experiments, analyzed data, designed the figures, and wrote the paper; R.M.K. performed experiments, analyzed data, and edited the paper; M.J.O. designed research, performed experiments, and analyzed data; Q.Z. performed experiments and analyzed data; L.X. isolated MAPCs; A.P.-M. and P.A.T. designed research; J.T. designed, organized, and supervised research; and B.R.B. designed, organized, and supervised research and edited the paper.

Conflict-of-interest disclosure: The authors declare no competing financial interests.

Correspondence: Bruce R. Blazar, University of Minnesota Masonic Cancer Center and Department of Pediatrics, Division of Bone Marrow Transplantation, MMC 109, 420 Delaware St SE, Minneapolis, MN 55455; e-mail: blaza001@umn.edu.

References

1. Fibbe WE, Nauta AJ, Roelofs H. Modulation of immune responses by mesenchymal stem cells. *Ann N Y Acad Sci*. 2007;1106:272-278.
2. Uccelli A, Moretta L, Pistoia V. Immunoregulatory function of mesenchymal stem cells. *Eur J Immunol*. 2006;36:2566-2573.
3. Rasmusson I, Ringden O, Sundberg B, Le Blanc K. Mesenchymal stem cells inhibit lymphocyte proliferation by mitogens and alloantigens by different mechanisms. *Exp Cell Res*. 2005;305:33-41.
4. Di Nicola M, Carlo-Stella C, Magni M, et al. Human bone marrow stromal cells suppress T-lymphocyte proliferation induced by cellular or nonspecific mitogenic stimuli. *Blood*. 2002;99:3838-3843.
5. Meisel R, Zibert A, Laryea M, Gobel U, Daubener W, Dilloo D. Human bone marrow stromal cells inhibit allogeneic T-cell responses by indoleamine 2,3-dioxygenase-mediated tryptophan degradation. *Blood*. 2004;103:4619-4621.
6. Sato K, Ozaki K, Oh I, et al. Nitric oxide plays a critical role in suppression of T-cell proliferation by mesenchymal stem cells. *Blood*. 2007;109:228-234.
7. Aggarwal S, Pittenger MF. Human mesenchymal stem cells modulate allogeneic immune cell responses. *Blood*. 2005;105:1815-1822.
8. Di Ianni M, Del Papa B, De Ioanni M, et al. Mesenchymal cells recruit and regulate T regulatory cells. *Exp Hematol*. 2008;36:309-318.
9. Augello A, Tasso R, Negrini SM, et al. Bone marrow mesenchymal progenitor cells inhibit lymphocyte proliferation by activation of the programmed death 1 pathway. *Eur J Immunol*. 2005;35:1482-1490.
10. Yañez R, Lamana ML, Garcia-Castro J, Colmenero I, Ramirez M, Bueren JA. Adipose tissue-derived mesenchymal stem cells have in vivo immunosuppressive properties applicable for the control of the graft-versus-host disease. *Stem Cells*. 2006;24:2582-2591.
11. Tisato V, Naresch K, Girdlestone J, Navarrete C, Dazzi F. Mesenchymal stem cells of cord blood origin are effective at preventing but not treating graft-versus-host disease. *Leukemia*. 2007;21:1992-1999.
12. Sudres M, Norol F, Trenado A, et al. Bone marrow mesenchymal stem cells suppress lymphocyte proliferation in vitro but fail to prevent graft-versus-host disease in mice. *J Immunol*. 2006;176:7761-7767.
13. Jiang Y, Jahagirdar BN, Reinhardt RL, et al. Pluripotency of mesenchymal stem cells derived from adult marrow. *Nature*. 2002;418:41-49.
14. Jiang Y, Vaessen B, Lenvik T, Blackstad M, Reyes M, Verfaillie CM. Multipotent progenitor cells can be isolated from postnatal murine bone marrow, muscle, and brain. *Exp Hematol*. 2002;30:896-904.
15. Bruder SP, Jaiswal N, Haynesworth SE. Growth kinetics, self-renewal, and the osteogenic potential of purified human mesenchymal stem cells during extensive subcultivation and following cryopreservation. *J Cell Biochem*. 1997;64:278-294.
16. Deans RJ, Moseley AB. Mesenchymal stem cells: biology and potential clinical uses. *Exp Hematol*. 2000;28:875-884.
17. Tolar J, Osborn M, Bell S, et al. Real-time in vivo imaging of stem cells following transgenesis by transposition. *Mol Ther*. 2005;12:42-48.
18. Gudmundsdottir H, Wells AD, Turka LA. Dynamics and requirements of T-cell clonal expansion in vivo at the single-cell level: effector function is linked to proliferative capacity. *J Immunol*. 1999;162:5212-5223.
19. Song HK, Noorchashm H, Lieu YK, et al. In vivo MLR: a novel method for the study of alloimmune responses. *Transplant Proc*. 1999;31:834-835.
20. Blazar BR, Taylor PA, McElmurry R, et al. Engraftment of severe combined immune deficient mice receiving allogeneic bone marrow via in utero or postnatal transfer. *Blood*. 1998;92:3949-3959.
21. Breyer A, Estharabadi N, Oki M, et al. Multipotent adult progenitor cell isolation and culture procedures. *Exp Hematol*. 2006;34:1596-1601.
22. Tolar J, O'Shaughnessy MJ, Panoskaltis-Mortari A, et al. Host factors that impact the biodistribution and persistence of multipotent adult progenitor cells. *Blood*. 2006;107:4182-4188.
23. Prevosto C, Zancollini M, Canevali P, Zocchi MR, Poggi A. Generation of CD4⁺ or CD8⁺ regulatory T-cells upon mesenchymal stem cell-lymphocyte interaction. *Haematologica*. 2007;92:881-888.
24. Casiraghi F, Azzollini N, Cassis P, et al. Pretransplant infusion of mesenchymal stem cells prolongs the survival of a semiallogeneic heart transplant through the generation of regulatory T-cells. *J Immunol*. 2008;181:3933-3946.
25. Ponomaryov T, Peled A, Petit I, et al. Induction of the chemokine stromal-derived factor-1 following DNA damage improves human stem cell function. *J Clin Invest*. 2000;106:1331-1339.
26. Takahashi HK, Iwagaki H, Yoshino T, et al. Prostaglandin E₂ inhibits IL-18-induced ICAM-1 and B7.2 expression through EP2/EP4 receptors in human peripheral blood mononuclear cells. *J Immunol*. 2002;168:4446-4454.
27. Harris SG, Padilla J, Koumas L, Ray D, Phipps RP. Prostaglandins as modulators of immunity. *Trends Immunol*. 2002;23:144-150.
28. Ruggeri P, Nicocia G, Venza I, Venza M, Valenti A, Teti D. Polyamine metabolism in prostaglandin E₂-treated human T lymphocytes. *Immunopharmacol Immunotoxicol*. 2000;22:117-129.
29. Brown DM, Warner GL, Ales-Martinez JE, Scott DW, Phipps RP. Prostaglandin E₂ induces apoptosis in immature normal and malignant B lymphocytes. *Clin Immunol Immunopathol*. 1992;63:221-229.
30. Ikegami R, Sugimoto Y, Segi E, et al. The expression of prostaglandin E receptors EP2 and EP4 and their different regulation by lipopolysaccharide in C3H/HeN peritoneal macrophages. *J Immunol*. 2001;166:4689-4696.
31. Harizi H, Juzan M, Grosset C, Rashedi M, Gualde N. Dendritic cells issued in vitro from bone marrow produce PGE₂ that contributes to the immunomodulation induced by antigen-presenting cells. *Cell Immunol*. 2001;209:19-28.
32. Krause P, Bruckner M, Uermosi C, Singer E, Groettrup M, Legler DF. Prostaglandin E₂ enhances T-cell proliferation by inducing the costimulatory molecules OX40L, CD70, and 4-1BBL on dendritic cells. *Blood*. 2009;113:2451-2460.
33. Li H, Guo Z, Jiang X, Zhu H, Li X, Mao N. Mesenchymal stem cells alter migratory property of T and dendritic cells to delay the development of murine lethal acute graft-versus-host disease. *Stem Cells*. 2008;26:2531-2541.
34. Fitzpatrick FA, Aguirre R, Pike JE, Lincoln FH. The stability of 13,14-dihydro-15 keto-PGE₂. *Prostaglandins*. 1980;19:917-931.
35. Pabst R, Westermann J. The role of the spleen in lymphocyte migration. *Scanning Microsc*. 1991;5:1075-1079; discussion 1079-1080.
36. Anderson BE, Taylor PA, McNiff JM, et al. Effects of donor T-cell trafficking and priming site on graft-versus-host disease induction by naive and memory phenotype CD4 T-cells. *Blood*. 2008;111:5242-5251.
37. Beilhack A, Schulz S, Baker J, et al. Prevention of acute graft-versus-host disease by blocking T-cell entry to secondary lymphoid organs. *Blood*. 2008;111:2919-2928.
38. Clouthier SG, Ferrara JL, Teshima T. Graft-versus-host disease in the absence of the spleen after allogeneic bone marrow transplantation. *Transplantation*. 2002;73:1679-1681.
39. Taylor PA, Panoskaltis-Mortari A, Swedin JM, et al. L-Selectin^{hi} but not the L-selectin^{lo} CD4⁺25⁺ T-regulatory cells are potent inhibitors of GVHD and BM graft rejection. *Blood*. 2004;104:3804-3812.
40. Ermann J, Hoffmann P, Edinger M, et al. Only the CD62L⁺ subpopulation of CD4⁺CD25⁺ regulatory T-cells protects from lethal acute GVHD. *Blood*. 2005;105:2220-2226.
41. Wysocki CA, Jiang Q, Panoskaltis-Mortari A, et al. Critical role for CCR5 in the function of donor CD4⁺CD25⁺ regulatory T-cells during acute graft-versus-host disease. *Blood*. 2005;106:3300-3307.
42. Zhang N, Schröppel B, Lal G, et al. Regulatory T-cells sequentially migrate from inflamed tissues to draining lymph nodes to suppress the alloimmune response. *Immunity*. 2009;30:458-469.
43. Aranguren XL, McCue JD, Hendrickx B, et al. Multipotent adult progenitor cells sustain function of ischemic limbs in mice. *J Clin Invest*. 2008;118:505-514.
44. Pelacho B, Nakamura Y, Zhang J, et al. Multipotent adult progenitor cell transplantation increases vascularity and improves left ventricular function after myocardial infarction. *J Tissue Eng Regen Med*. 2007;1:51-59.
45. Tolar J, Wang X, Braunlin E, et al. The host immune response is essential for the beneficial effect of adult stem cells after myocardial ischemia. *Exp Hematol*. 2007;35:682-690.
46. Kovacs-Bankowski M, Streeter PR, Mauch KA, et al. Clinical scale expanded adult pluripotent stem cells prevent graft-versus-host disease. *Cell Immunol*. 2009;255:55-60.
47. Ghansah T, Paraiso KH, Highfill S, et al. Expansion of myeloid suppressor cells in SHIP-deficient mice represses allogeneic T-cell responses. *J Immunol*. 2004;173:7324-7330.